

PACS numbers: 42.25.Fx; 42.25.Gy; 78.67.–n
DOI: 10.1070/QE2011v041n06ABEH014539

Photonic nanojet effect in multilayer micrometre-sized spherical particles

Yu.E. Geints, A.A. Zemlyanov, E.K. Panina

***Abstract*. The spatial and amplitude characteristics of photonic nanojets from micrometre-sized composite particles consisting of a nucleus and several shells with different refractive indices were considered. We investigated the longitudinal and transverse dimensions of the photon jet as well as the dependence of its peak intensity on the optical contrast of the shells. It was shown that, by varying the refractive index of the neighbouring shells in composite spherical microparticles, it is possible to manipulate the photonic nanojet parameters, in particular, increase its length or raise the peak intensity of the photon flux.**

Keywords: *multilayer spherical targets, Mie scattering, photonic nanojet, optical contrast of a layer.*

1. Introduction

A 'photonic nanojet' (PNJ) is a narrow high-intensity light beam formed in the immediate vicinity of a shadow surface of transparent dielectric symmetric bodies (spheres, cylinders) with diameter of the order of or somewhat greater than the wavelength of the light radiation incident on them. The PNJ is essentially the exterior focal region of the light wave diffracted by the transparent particle, this region being several in-medium wavelengths long. The PNJ's occurrence is due to constructive interference of the light fields of the radiation scattered by and transmitted through the particle. In this case, a special feature of the PNJ is a rather high spatial localisation of the light field in the direction which is perpendicular to the direction of radiation incidence, resulting in the subwavelength size of the photon flux.

Attention to the effect of PNJ formation was first drawn by Chen et al. [1] in the study of the spatial near-field structure in the scattering of a light beam from a transparent quartz micrometre-sized cylinder. The modern state of the problem has been recently reviewed by Heifetz et al. [2].

The interest in this effect is primarily due to the prospect of its practical use in nanophotonics, biology, medicine, nanoelectronics, and data storage systems. Several authors reported the potentiality of designing sensors with a high (nanometer-scale) spatial resolution on the basis of the PNJ phenomenon [3, 4], as well as of making an 'optical knife' for precision surgery [5] and 'optical tweezers' for manipulating individual nanoobjects [6]. Also possible is the development of optical data storage devices with an ultrahigh density information recording [7] and technology for direct-write nanopatterning of photosensor surfaces [8]. The principles of operation of the above devices rely on the fact that a PNJ, firstly, can provide a high-intensity electromagnetic field in a fixed spatial domain near a microparticle and, secondly, is highly sensitive to different kinds of perturbations, both of field and material nature. For instance, when some micro- or nanoobject finds its way to the domain of the photon flux, the PNJ interacts with it, which may lead to changes in the optical properties of the 'parent' microsphere itself. In particular, this may have the effect that the amplitude of its backscattering signal will be enhanced by several orders of magnitude in comparison with the case of backscattering from an isolated microsphere [4]. This all brings to the foreground the problem of controlling the PNJ parameters – the necessity of controllable variation in PNJ size and intensity for the optimal solution of the task facing a specific device.

The most important characteristics (the lateral dimension, the length, the peak intensity) of PNJs formed near uniform dielectric microspheres and microcylinders irradiated by a laser beam were studied in several theoretical papers [9 – 12]. These investigations revealed that the spatial form and intensity of the PNJs experience significant changes under variation in the size and optical properties of the microparticle. Furthermore, using for PNJ production, instead of a uniform microsphere, a composite microparticle comprising a nucleus and one or several shells with refractive indices different from that of the 'parent' sphere makes it possible to significantly deform the photon flux characteristics, in particular, to anomalously lengthen the PNJ [13 – 15]. The main idea is to maximally reduce the contrast of refractive index for the incident radiation at the outer particle boundary by way of a gradual lowering of the optical density of the shells, beginning from the microsphere nucleus. Realised in this case is a softer focusing of the optical wave field by the multilayer particle in comparison with a uniform sphere.

It is pertinent to note that the multilayer microspheres considered below are in fact the so-called optical systems with a graded refractive index, whose most important examples are the Maxwell (fisheye) and Luneburg lenses [16]. These lens systems are also characterised by the radial

Yu.E. Geints, A.A. Zemlyanov, E.K. Panina V.E. Zuev Institute of Atmospheric Optics, Siberian Branch, Russian Academy of Sciences, pl. Akad. Zueva, 1, 634021 Tomsk, Russian Federation;
e-mail: ygeints@iao.ru, zaa@iao.ru, pek@iao.ru

Received 17 January 2011; revision received 16 March 2011
Kvantovaya Elektronika **41** (6) 520 – 525 (2011)
Translated by E.N. Ragozin

lowering of the refractive index from the centre to the periphery and, in particular, are employed in photography and radiophysics.

In Refs [13, 14] a study was made of the photon fluxes from dielectric particles 2 and 5 μm in radius irradiated by visible light, which consisted of five or more concentric layers (up to a hundred, including the nucleus). The refractive index n of each layer varied with number: the nucleus was optically more dense than the outer shell. It was noted that this radial stepwise variation in n enabled to lengthen the PNJ length up to 20 μm ($\sim 40\lambda$) under certain conditions. However, this was achieved at the expense of a PNJ broadening in the lateral direction and a PNJ intensity lowering.

However, the papers cited above made use of one and the same type of layerwise variation in the refractive index of particles, namely, the linear variation with layer number. This brings up the question: How will the PNJ parameters be affected by another type of variation in the refractive index in going from layer to layer? This circumstance became the incentive for carrying out additional investigations; its results are outlined in the present paper.

Therefore, the main objective of this paper is to consider the PNJ characteristics for a wider class of multilayer spherical microparticles, which differ by the type of variation in the optical properties of the neighbouring shells. Proceeding from numerical calculations, which were performed in the framework of the Mie theory modified for the case of scattering by multilayer spheres, we investigated the transverse and longitudinal dimensions as well as the peak intensity of the PNJs from layered non-absorptive dielectric microspheres of different diameter residing in the air. We determined the condition whereby it is possible to either lengthen the PNJ or raise the peak intensity of the photon flux.

2. Model of a composite particle and Mie theory for a multilayer sphere

We consider a micrometre-sized particle consisting of a nucleus of radius a_0 and some number N of concentric layers of equal thickness h and radii a_s ($s = 0, \ldots, N$, see Fig. 1). Each sth layer of the composite particle is optically uniform and is characterised by its own refractive index n_s (the layer is non-absorptive). Let the particle be in the air (with refractive index $n_\infty = 1$) and be illuminated by a plane monochromatic wave $\boldsymbol{E}_i = E_0 \boldsymbol{e}_x \exp(\mathrm{i}\omega z/c)$ polarised along the x axis and propagating along the z axis (c is the speed of light in vacuum).

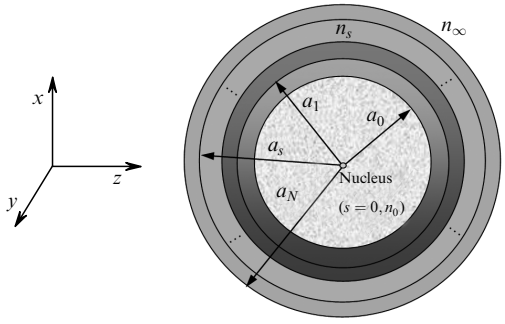

Figure 1. Multilayer spherical particle model.

To calculate the spatial structure of the optical fields in the vicinity of a multilayer spherical particle, we take advantage of the so-called modified Mie theory for multilayer spheres [17]. In the framework of this theory, the optical fields in every layer of the particle are written in the form of classical Mie series with expansion coefficients, which are determined by solving the corresponding boundary conditions. In this case, the total field in each layer is represented as the sum of the wave fields diffracted by the previous layer and the wave from the layer which is exterior relative to the given one. Therefore, in the spherical system of coordinates the vectors of electric ($\boldsymbol{E}_s$) and magnetic ($\boldsymbol{H}_s$) fields [$\boldsymbol{r} = (e, \theta, \varphi)$] in the sth layer are written in the following universal form [15]:

$$\begin{aligned}
\boldsymbol{E}_s(\boldsymbol{r}) &= \sum_{n=1}^{\infty} E_n \Big[\mathrm{i}\Big(a_n^s \boldsymbol{N}_{\mathrm{e}1n}^{(3)}(\boldsymbol{r}) - d_n^s \boldsymbol{N}_{\mathrm{e}1n}^{(1)}(\boldsymbol{r}) \Big) \\
&\quad - \Big(b_n^s \boldsymbol{M}_{\mathrm{o}1n}^{(3)}(\boldsymbol{r}) - c_n^s \boldsymbol{M}_{\mathrm{o}1n}^{(1)}(\boldsymbol{r}) \Big) \Big], \\
\boldsymbol{H}_s(\boldsymbol{r}) &= \frac{k_s}{\omega} \sum_{n=1}^{\infty} E_n \Big[\mathrm{i}\Big(b_n^s \boldsymbol{N}_{\mathrm{o}1n}^{(3)}(\boldsymbol{r}) - c_n^s \boldsymbol{N}_{\mathrm{o}1n}^{(1)}(\boldsymbol{r}) \Big) \\
&\quad + \Big(a_n^s \boldsymbol{M}_{\mathrm{e}1n}^{(3)}(\boldsymbol{r}) - d_n^s \boldsymbol{M}_{\mathrm{e}1n}^{(1)}(\boldsymbol{r}) \Big) \Big],
\end{aligned} \tag{1}$$

where $\boldsymbol{M}_{\mathrm{e(o)}mn}^{(l)}$ and $\boldsymbol{N}_{\mathrm{e(o)}mn}^{(l)}$ are the even (e) and odd (o) vector spherical harmonics [18] of orders $l = 1$ and 3 (for a plane wave, $m = 1$); $k_s = n_s\omega/c$ is the modulus of the wave vector in the layer with refractive index n_s; and $E_n = E_0 \mathrm{i}^n \times (2n+1)/[n(n+1)]$. It is assumed that $s = 0$ for the particle nucleus and that $s = N + 1$ for the space surrounding the particle. Therefore, a completely uniform particle in this notation is the particle with the zero number of layers ($N = 0$).

The arrays of partial amplitudes a_n^s, b_n^s, c_n^s, and d_n^s of expansion (1) are expressed in terms of the generalised coefficients A_n^s, B_n^s, C_n^s, and D_n^s by the following formulas:

$$a_n^s = A_n^s, \quad b_n^s = B_n^s, \quad c_n^s = D_n^s + 2B_n^s, \quad d_n^s = C_n^s + 2A_n^s.$$

The exceptions are the nucleus ($s = 0$), where $a_n^0 = b_n^0 = 0$, $c_n^0 = C_n^0$, and $d_n^0 = D_n^0$, and the outer domain ($s = N + 1$), where we should set $a_n^{N_s+1} = -A_n^{N_s+1}$, $b_n^{N_s+1} = -B_n^{N_s+1}$, and $c_n^{N_s+1} = d_n^{N_s+1} = 1$. The coefficients $A_n^s - D_n^s$ are determined by calculating the recursion

$$A_n^s = U_n^{s-1} C_n^s, \quad B_n^s = V_n^{s-1} D_n^s, \quad C_n^s = \prod_{t=s}^{N} P_n^t, \quad D_n^s = \prod_{t=s}^{N} Q_n^t$$

with the initial conditions $C_n^{N+1} = D_n^{N+1} = 1$. The auxiliary functions U_n^s, V_n^s, P_n^s, and Q_n^s are expressed in terms of the Riccati–Bessel functions and calculated by the corresponding recurrence formulas [17].

To specify the refractive index of each layer we introduce the following functional relationship:

$$\frac{n_s}{n_0} = \left(\frac{n_N}{n_0} \right)^{(s/N)^g}. \tag{2}$$

In this formula the parameter $g > 0$ defines the radial variation in the optical contrast $\gamma_s = n_s/n_{s+1} + 1 = h(n_0/n_N)^{[(s+1)^g - s^g]/N^g}$ of the layers, beginning with the optically most 'dense' nucleus (n_0) and ending with the outer shell with a lower refractive index than that of the

nucleus ($n_N < n_0$). For definiteness, in what follows we shall consider particles with four external shells ($N = 4$) and with fixed refractive indices of the nucleus and the outer shell: $n_0 = 1.5$, $n_N = 1.1$. The shell thicknesses are assumed to be equal to the radius of the nucleus ($h = a_0$).

Here it is pertinent to note that this selection of the n_0 and n_N values is partly due to the real capabilities of the presently existing technology of fabrication of thin shells with varied refractive indices on microobjects [19, 20]. On the other hand, restricting our PNJ consideration to only particles with $N = 4$ should not have a significant effect on the generality of the results obtained in our work, because the effect of the number of layers on the characteristics of a photonic jet has already been considered by Kong et al. [13]. They showed that the smoothness of radial variation in the refractive index of a multilayer particle from the centre to the periphery, which is achieved by raising the number shells, has no appreciable effect on the dimensional parameters of the resultant PNJ, and their investigation may well be restricted to a sphere with several layers of equal thickness.

Figure 2 shows the dependences of the refractive index on the relative radial coordinate r/a_N, which correspond to the main types of spherical shell particles studied in our work; these particles differ by the character of variation in the contrast γ_s. One can see that particles with $g < 1$ (type I) are characterised by a smoother variation in the refractive index between the neighbouring layers. There actually occurs an increase of the total thickness of the outer (less 'dense') particle shell relative to the size of the 'dense' nucleus. At the same time, the difference in n values between the nucleus and the first shell layer of the particle increases, which manifests itself in a sharp rise of the optical contrast between them (see curve for $g = 0.2$ in Fig. 2b). In the case of realisation of this particle morphology, clearly the influence of the shell on the PNJ parameters will be dominant.

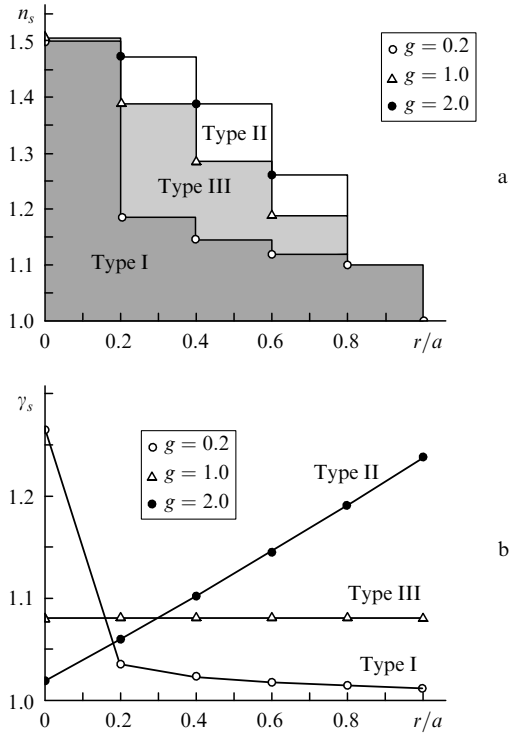

Figure 2. Radial variation in the refractive index n_s (a) and the optical contrast γ_s (b) between the neighbouring layers of a multilayer particle for different g values.

When $g > 1$ (type-II particles), the optical contrast of the layers, as follows from Fig. 2a, rises with their number, i.e. the effective radius of the 'dense' nucleus lengthens and the thickness of the less 'dense' shell shortens. This has the effect that the main part in the transformation of the photon flux inside such a multilayer particle will be played by precisely the nucleus. For $g \gg 1$, in its optical properties the multilayer particle therefore approaches a uniform particle of longer radius than the nucleus, a particle of size a_N ($a_N > a_0$) with a high refractive index ($n \to n_0$).

For $g = 1$ (type III), the refractive index varies linearly from layer to layer, like in Refs [13, 14], while the contrast parameter $\gamma_s = (n_0/n_N)^{1/N}$ remains invariable.

3. Results and their discussion

The influence of the morphological type of the particle's optical nonuniformity on the PNJ shape is shown in Fig. 3, which depicts two-dimensional as well as their corresponding radial and transverse distributions of the relative optical field intensity $B(x,z) = |E(x,z)|^2/E_0^2$ at the principal section of the multilayer spherical particle for different values of g. Shown for comparison in the same drawing are the versions of jet formation from uniform spheres of the same diameter and with the same refractive indices as in the outer shell (Fig. 3a) and the nucleus (Fig. 3e).

One can see that the spatial configuration of the photon flux depends essentially on the character of radial variation in the optical contrast in the particle. Characteristic for type-I particles with a gradually lowering contrast between the shells ($g = 0.2$, Fig. 3b) is a lengthy low-intensity PNJ of length $\sim 10\lambda$, which is hardly different in shape from that for a uniform sphere with $n = 1.1$ (Fig. 3a).

For type-II particles ($g = 2$, Fig. 3d) it is valid to say that instead of a photonic jet there forms a spherically shaped field 'blob' at the particle's shadow surface. In this case, its intensity is several times the highest intensity of the PNJ in the previous case, and the longitudinal and transverse dimensions amount to about 1 μm. Appropriate here is a qualitative analogy with the aforementioned spherical Luneburg lens, which focuses any incident parallel beam to a point on its opposite surface. Concerning the multilayer sphere with $g = 2$ under our consideration, the radial variation in its refractive index closely replicates the profile of the refractive index of the Luneburg lens, which may be represented in the generalised form as follows:

$$n(r) = n_0 \sqrt{n_0^2 - n_N^2 \left(\frac{r}{a_N}\right)^2}.$$

A perfect focal spot on the rear particle surface is not formed, because the Luneburg solution was obtained in the framework of geometrical optics with neglect of diffraction effects, which are significant for optically small particles.

The features of both of the cases considered above are combined in the configuration of the PNJ of a particle with a constant interlayer optical contrast (type III, $g = 1$, Fig. 3c). In particular, there is a region of high field intensity near the rear hemisphere, which is somewhat larger and lower in intensity than in Fig. 3d, as well as a rather lengthy

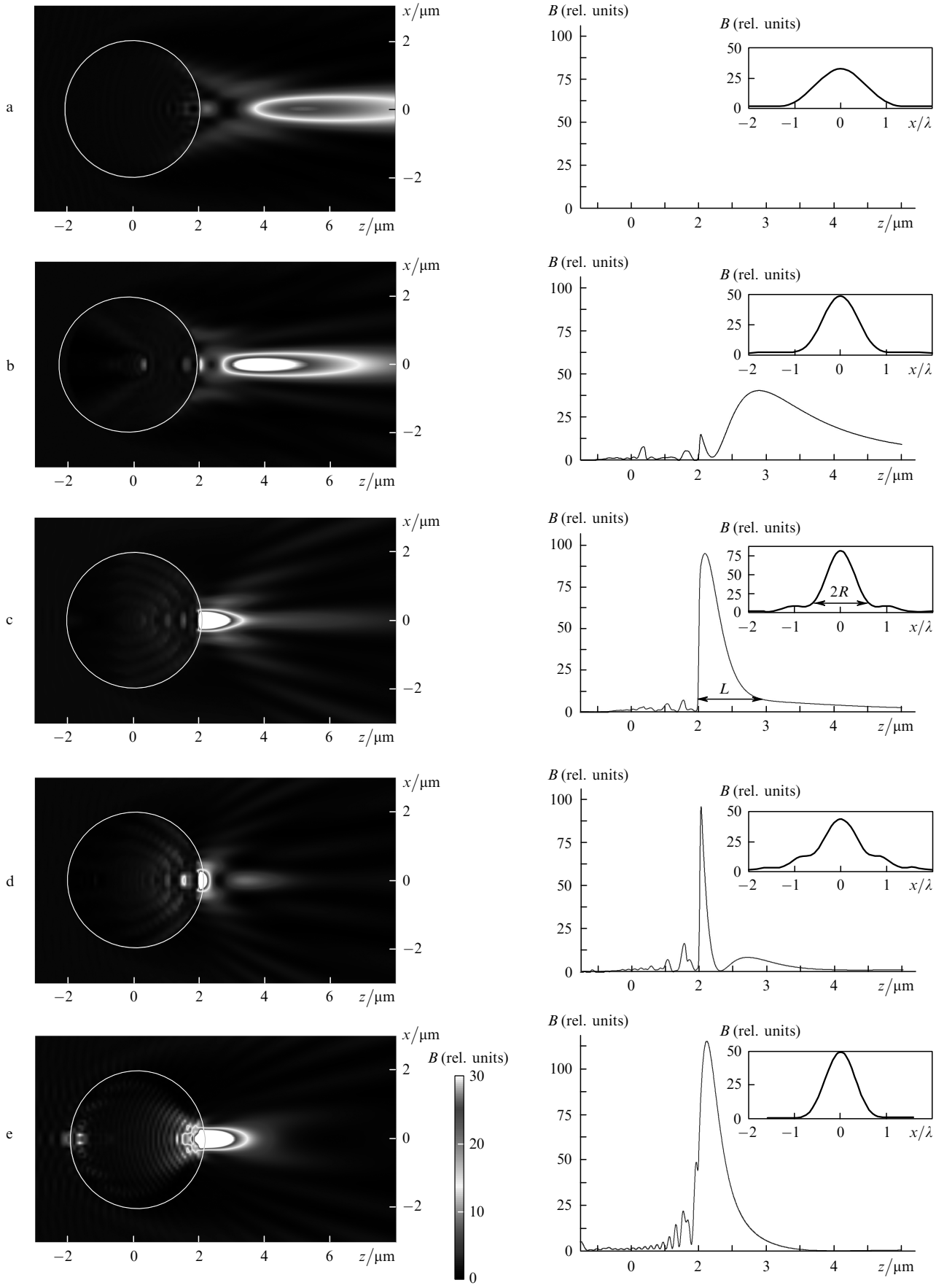

Figure 3. Two-dimensional and radial distributions of the relative intensity of the light field in the vicinity of spherical particles with different internal structure and $a_N = 2$ μm ($N = 4$, $h = 0.4$ μm) illuminated by 0.532-μm radiation (incident from the left) as well as their cross sections; uniform particle with $n = 1.1$ (a) and 1.5 (e) and five-layer particle with $g = 0.2$ (b), 1 (c), and 2 (d). The insets show the transverse PNJ profile.

'tail', in which $B \approx 10$. Interestingly, achieved with this structural particle type is the smallest – among the version considered – lateral width (at half-height in intensity) of the photon flux, which does not exceed the wavelength of incident radiation.

A comparison of Figs 3b – 3d shows that the type of a multilayer particle determines not only the PNJ dimension and intensity, but also the separation of the PNJ from the surface. For small values of the g parameter, the resultant PNJ is detached from the shadow hemisphere, which has an adverse effect on its power characteristics. With increasing g, the coordinate of the its intensity peak approaches the particle to 'stick' to the outer surface of the sphere, emanating from this surface in the form of an exponentially decaying tail.

To quantitatively characterise the PNJ shape we introduce its three parameters [15]: the peak intensity B_{max}, the effective length L and the transverse size R calculated at a level $1/e^2$ of the peak intensity (see Fig. 3c). The dependences of these characteristics on the structural parameter g are plotted in Fig. 4.

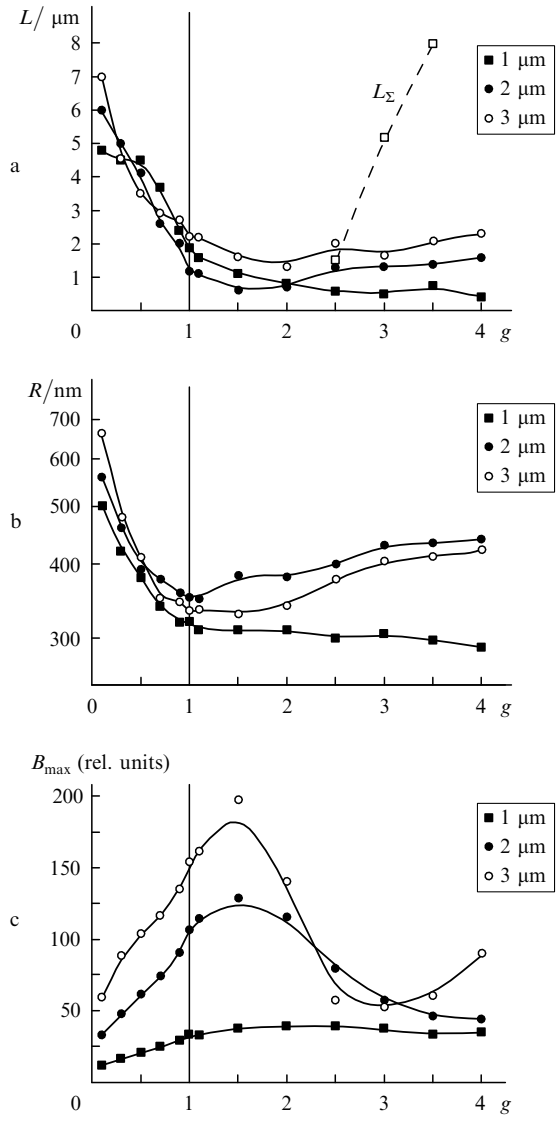

Figure 4. Parameters of the PNJs of multilayer particles of different radius in the air ($\lambda = 0.532$ μm).

As expected, the photon jet formed in the near-field zone of the particles with a lowering optical contrast between the shells ($g < 1$) is longest, but has a low intensity and is broad in the transverse direction. The highest PNJ intensity is realised for particles with a radial variation in the refractive index close to the linear dependence ($g \approx 1 - 1.5$), the jet's halfwidth R being smaller than the diffraction limit in this range of g parameter variation: $R < R_d$, where $R_d = n_\infty \lambda/\sqrt{2}$ is the minimal radius of the focal waist of the focused light beam (at a level of $1/e^2$).

In multilayer type-II particles ($g > 1$) the PNJ length stabilises at a level of several micrometres (depending on the initial particle size). The intensity of the photon jet from the particle becomes lower and its width increases. Furthermore, the very PNJ structure becomes more complicated. With reference to Fig. 3d, apart from the primary intensity peak located at the particle surface, in the radial direction there appears the secondary field blob spaced at ~ 1 μm from the first one. This 'light bullet' is less intense ($B \sim 10$), but it is much longer than the primary PNJ. The total length L_Σ of such a combined photonic jet for a particle with $a =$ 2 μm is shown with empty squares in Fig. 4a. One can see that it may be quite significant.

Kong et al. [13] proposed a peculiar quality criterion $Q = B_{max} L/R$ for characterising PNJs. This characteristic reflects, though very relatively, the efficiency of applying a PNJ for the solution of practical problems, because the Q factor rises with increasing intensity and length of the photonic jet and with decreasing its cross section.

The PNJ quality criterion normalised to its peak value is plotted in Fig. 5 in relation to the structural particle shell parameter. The points in this Figure correspond to different structural versions of composite particles for which we obtained computational data on PNJ parameters. For clarity these points are connected by spline interpolation. It turned out that the Q parameter attains its highest values for $g \approx 0.5$, i.e. in type-I rather than in type-II particles. Consequently, it is this morphological type of multilayer particles that most optimally combines the high spatial localisation of the optical field of the photonic jet and the relatively high level of its intensity. By the way, the quality criterion of the PNJ of completely uniform particles ($N = 0$ and $g \to 0$ or $g \to \infty$), whose optical field distribution is depicted in Figs 3a and 3e, is equal to ~ 0.8 in both cases.

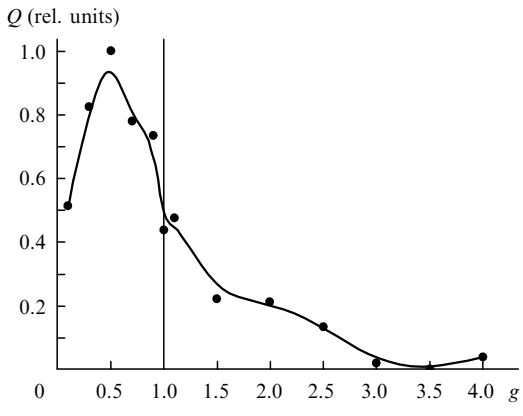

Figure 5. Normalised quality criterion of the PNJs of particles with $a = 2$ μm and different internal shell structure.

4. Conclusions

Therefore, in this work we considered the main characteristics of the photonic nanojets (the transverse dimension, the length, and the peak intensity) formed by transparent dielectric microspheres irradiated by a laser beam. This investigation covers the morphological class of particles optically nonuniform in the radial direction, which are a spherical nucleus with equally thick concentric shells with different refractive indices deposited on it. Numerical calculations were performed in the framework of the modified Mie theory for the radiation scattering by multilayer spheres. We have clearly shown that it is possible to control the photonic nanojet parameters by varying the optical contrast between the particle shells.

Acknowledgements. This work was supported by the Physical Sciences Division of the Russian Academy of Sciences.

References

1. Chen Z., Taflove A., Backman V. *Opt. Express*, **12**, 1214 (2004).
2. Heifetz A., Kong S.-C., Sahakiana A.V., Taflove A., Backman V.J. doi: 10.1166/jctn.2009.1254. 1979 (2009).
3. Utzinger U., Richards-Kortum R.R. *J. Biomed. Opt*., **8**, 121 (2003).
4. Li X., Chen Z., Taflove A., Backman V. *Opt. Express*, **13**, 526 (2005).
5. Astratov V.N., Darafsheh A., Kerr M.D., Allen K.W., Fried N.M., Antoszyk A.N., Ying H.S. doi: 10.1117/2.1201002.002578 (2010).
6. Cui X, Erni D, Hafner C. *Opt. Express*, **16**, 13560 (2008).
7. Kong S.-C., Sahakian A.V., Heifetz A., Taflove A., Backman V. *Appl. Phys. Lett*., **92**, 211102 (2008).
8. Wu W., Katsnelson A., Memis O.G., Mohseni H. *Nanotechnol*., **18**, 485302 (2007).
9. Itagi A.V., Challener W.A. *J. Opt. Soc. Am. A*, **22**, 2847 (2005).
10. Heifetz A., Simpson J.J., Kong S.-C., Taflove A., Backman V. *Opt. Express*, **15**, 17334 (2007).
11. Devilez A., Stout B., Bonod N., Popov E. *Opt. Express*, **16**, 14200 (2008).
12. Devilez A., Bonod N., Stout B., Gerard D., Wenger J., Rigneault H., Popov E. *Opt. Express*, **17**, 2089 (2009).
13. Kong S.-C., Taflove A., Backman V. *Opt. Express*, **17**, 3722 (2009).
14. Ruiz C.M., Simpson J.J. *Opt. Express*, **18**, 16805 (2010).
15. Geints Yu.E., Zemlyanov A.A., Panina E.K. *Opt. Spektrosk*., **109**, 643 (2010).
16. Born M., Wolf E. *Principles of Optics* (Oxford: Pergamon Press, 1969; Moscow: Nauka, 1973).
17. Xu H. *Phys. Rev. B*, **75**, 073405 (2005).
18. Bohren C.F., Huffman D.R. *Absorption and Scattering of Light by Small Particles* (New York: Wiley, 1983; Moscow: Mir, 1986).
19. Prodan E., Radloff C., Halas N.J., Nordlander P. *Science*, **302**, 419 (2003).
20. Poco J.F., Hrubesh L.W. U.S. Patent 6158244 (2008).